Geophysical Research Letters

RESEARCH LETTER
10.1029/2025GL116331

High-Spatial Resolution Space-Based Observations in the Upper Troposphere and Upper Mesosphere of Wavelike Features Produced by Hurricane Ian

J. H. Hecht[1], D. S. Nolan[2], L. J. Gelinas[1], and R. L. Walterscheid[1,3]

[1]Space Science Applications Laboratory, The Aerospace Corporation, El Segundo, CA, USA, [2]Rosenstiel School of Marine and Atmospheric, Earth Science, University of Miami, Miami, FL, USA, [3]Department of Physical Sciences, Embry-Riddle Aeronautical University, Daytona Beach, FL, USA

Key Points:

- H-band imagery reveals dynamics with high-spatial resolution at hurricane cloud tops and in the airglow independent of lunar illumination
- Short scale waves in the cloud imagery include structures that are consistent with secondary instabilities of Kelvin-Helmholtz Instabilities
- Gravity waves plausibly generated by dynamic processes at the Hurricane Ian eyewall

Correspondence to:
J. H. Hecht,
james.hecht@aero.org

Citation:
Hecht, J. H., Nolan, D. S., Gelinas, L. J., & Walterscheid, R. L. (2025). High-spatial resolution space-based observations in the upper troposphere and upper mesosphere of wavelike features produced by Hurricane Ian. *Geophysical Research Letters*, *52*, e2025GL116331. https://doi.org/10.1029/2025GL116331

Received 2 APR 2025
Accepted 30 AUG 2025

Author Contributions:
Conceptualization: J. H. Hecht
Data curation: L. J. Gelinas
Formal analysis: J. H. Hecht, D. S. Nolan
Investigation: J. H. Hecht, L. J. Gelinas
Methodology: J. H. Hecht, D. S. Nolan, L. J. Gelinas, R. L. Walterscheid
Software: J. H. Hecht
Visualization: D. S. Nolan
Writing – original draft: J. H. Hecht, D. S. Nolan, L. J. Gelinas, R. L. Walterscheid

Abstract A new high-spatial resolution camera on the International Space Station used OH nightglow in the H-band to image the ground at an ~70 m pixel footprint over an ~280 km swath and maintained this resolution during its 1.5 s exposure. Near 0405 UT on 28 September 2022 moon down images obtained over the eyewall of the category 4 Hurricane Ian revealed short-horizontal wavelength (~5 km) instabilities with even finer scale (~1–2 km) perpendicular structures, similar to those identified in recent modeling. Images taken (~10 s apart) are used to separate these tropospheric features from atmospheric gravity waves (AGWs) imaged at ~87 km. Geostationary Operational Environmental Satellite 16 (GOES-16) data were used to estimate the altitudes of the tropospheric features. Available auxiliary data were used to show that the AGWs plausibly originated from close to Ian's eyewall 1–2 hr earlier.

Plain Language Summary Just before landfall of the category 4 Hurricane Ian around 0405 UT on 28 September 2022 a new and unique camera on the International Space Station was able to simultaneously capture at very high spatial resolution the wave structure near the top of the clouds at 12–17 km, and high above that at ~87 km, near the mesopause, the coldest region of the Earth's atmosphere. The high-altitude imagery is possible because the Earth's atmosphere naturally emits light at ~87 km that both illuminates the clouds below and is also affected by atmospheric gravity waves (AGWs), generated by the hurricane, that subsequently propagate to higher altitudes. This new imagery revealed very fine-scale instability structure in Ian's clouds never seen before at this resolution and AGWs at ~87 km that were generated about 1–2 hr earlier, probably by dynamic processes near the eyewall of the hurricane.

1. Introduction

Hurricanes are prolific generators of atmospheric gravity waves (AGWs) and associated wavelike instabilities and turbulence (Hoffmann et al., 2018; Nolan & Zhang, 2017; Wright, 2019). Their dynamics affect atmospheric structures at the hurricane cloud tops and at higher altitudes as the AGWs can propagate upwards to the mesosphere and lower thermosphere (MLT). The dynamical effects of these waves on atmospheric structure are not well understood because they often occur at fine horizontal scales of a few km, which until recently have not been accessible to imagery. Since hurricane-associated clouds preclude ground-based imagery of AGWs, space-based sensors, two of which are highlighted below, have been used to obtain hurricane-related imagery.

The legacy Geostationary Operational Environmental Satellite (GOES) platform has bands covering visible, near-infrared (NIR), and IR wavelengths that can be used to study tropospheric clouds. The visible daytime channels have 500 m pixel footprints while the IR channels, which can image at night, have 2 km footprints and observe thermal emission. This emission may not reveal the same fine-scale structure seen in visible band imagery that uses scattered light. We use GOES-16 data in this study.

The National Polar-Orbiting Partnership (NPP) is a newer system that allows extensive geographic coverage of tropospheric and in some cases MLT phenomena, the latter not seen by GOES. In particular, the day-night band (DNB), with a native pixel footprint of 750 m, is very sensitive to radiation from about 500 to 900 nm, including airglow emission originating above 80 km. Miller and colleagues have shown the utility of using DNB observations to study a number of mesospheric AGW phenomena related to tropical cyclones (Yue et al., 2014) as well as the Category 5 Hurricane Matthew (Miller et al., 2019; Xu et al., 2019). The issues with the DNB were

reviewed by Hecht et al. (2023) and revolve around the low intensity of the airglow emission. This makes observations only feasible when the airglow is brighter than normal, and when the moon is below the horizon (moon down) so that tropospheric cloud regions are not illuminated. In addition, as is also true for the GOES imagery, the pixel footprint precludes establishing the prevalence of features smaller than ∼1–2 km.

There is a new technique that overcomes the limitations of the DNB. The Phenomenology Imager and Nighttime Observer (PIANO) on the International Space Station (ISS) imaged the brighter OH airglow emission in the H-band (∼1.5 to 1.72 microns) that peaks near 87 km with a vertical extent of about 10 km. His airglow is nearly as bright as the light from the full moon, enabling PIANO to collect imagery, at all moon phases. PIANO captures images of the ground and clouds via reflected airglow, as well as imaging directly the airglow emission layer.

PIANO is an advanced version of the Near infrared Airglow Camera (NIRAC) which flew on the ISS from 2019 to 2021 (Gelinas et al., 2024; Hecht et al., 2023). PIANO's larger detector (4,096 × 4,096 pixels) allows a pixel footprint of approximately 70 m square at ground level decreasing to 55 m square at the 87 km airglow layer altitude when viewed from the ISS at 420 km. The field of view (FOV) is approximately 280 × 280 km at ground level and 220 × 220 km at 87 km altitude. In the analysis shown here images are generally binned by a factor of two to give effective pixel footprints of ∼130 m at 15 km altitude. For PIANO and NIRAC the pixel footprint is essentially constant over the detector because of its rectilinear optics. This is combined with a motion-compensation system for smear-free ground imaging over each ∼1.5 s exposure (Gelinas et al., 2024). The ∼10 s image cadence results in consecutive images seeing portions of the same region, allowing unambiguous retrieval (and separation) of ground and tropospheric cloud features from higher-altitude AGWs and Kelvin-Helmholtz Instabilities (KHIs) as detailed in Sections 3.1 and 3.2 of Hecht et al. (2023). This separation works even in the presence of optically thick clouds. A sequence of images also allows an estimate of a feature's velocity.

Just after 0400 UT September 28 (2300 LT September 27) 2022, PIANO images were obtained, with the moon down, as its FOV passed from Pensacola Florida to Jamaica, a path that included the fully developed eyewall of the Category 4 Hurricane Ian (Bucci et al., 2023) about 12 hr before landfall while it was moving to the northeast at ∼5 ms^{-1}. PIANO's imagery allows Ian's cloud features to be distinguished from several bright airglow-altitude AGW phase-fronts separated by about 25 km. We find that it is plausible that the AGWs originated from close to the Ian eyewall ∼1–2 hr earlier.

Smaller-scale wavelike features with horizontal wavelengths (λ_h) ∼5 km were observed at hurricane cloud top altitudes that are consistent with the recently identified "non-propagating" waves (NPWs) introduced by Nolan and Onderlinde (2022). They suggest that the NPWs are most likely KHIs. The very high spatial resolution of PIANO images reveal, for the first time, small-scale structures that are perpendicular to the primary NPW phase fronts and that are morphologically similar to KHI secondary structures seen in airglow imagery (Hecht, 2004; Hecht et al., 2014). These unique observations provide strong support for the modeling hypothesis that NPWs are KHIs.

2. Observations

2.1. PIANO Image Example

The PIANO image processing accounts for the increased pitch of the ISS during the observations. NIRAC image processing assumes that the detector is parallel to the ground and the ISS pitch of 1°-2° resulted in only minor post-processing to compensate for the less than 1% image stretch as described in Hecht et al. (2023). For PIANO observations the pitch approached 10°, distorting the image so that the stretch compensation was larger, above 5%. The other PIANO processing issues were (a) knowing the precise time of the image, that is uncertain by a few tenths of a second (a few ground km), affecting the geolocation of a pixel, and (b) accounting for the almost half a degree displacement of the center of the image, due to the pitch, from the ISS location. Having a clear view of the ground or of distinct Ian cloud features minimized these effects and allowed for corrections of these uncertainties in this study.

For this study it was fortunate that the first image, taken at 040343.00 (hhmmss.cc) UT included observations over Pensacola Florida. Figure 1a shows a map of the image sequence that included the Ian imagery. Figure 1b shows that the in first image a corner of the FOV included a clear view of Pensacola, Florida that confirmed proper

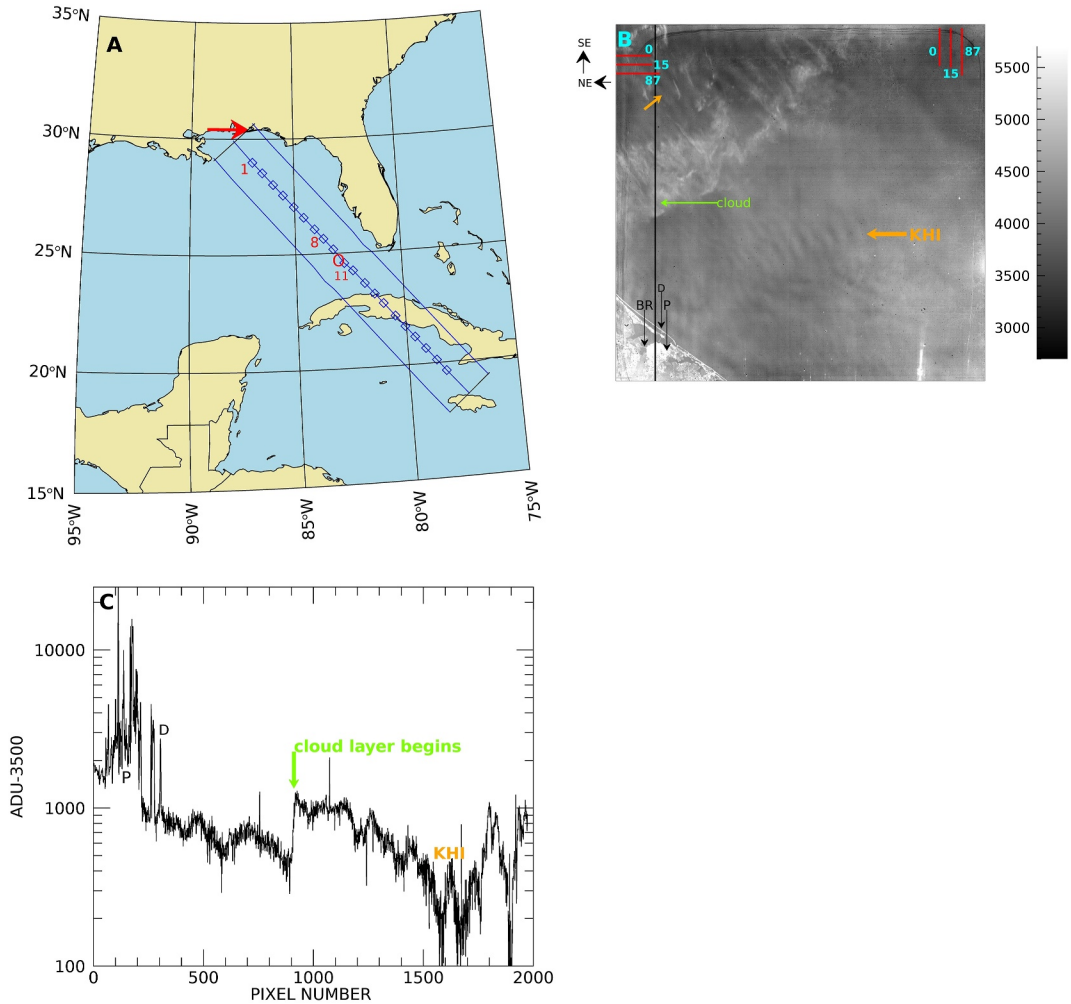

Figure 1. (a) Map with the approximate image centers (blue boxes). Images 1, 8, and 11 are marked. A red O marks the eye center and an arrow points to Pensacola. The FOV is the width between the blue lines and twice the distance from the first blue box to the blue end line. (b) Image 1 whose orientation is shown where SE (NE) is ~133° (223°) clockwise from North. The thick black line highlights features plotted in panel (c). The orange arrows show mesosphere KHIs. The green arrow points tropospheric clouds. The blue arrows point to Pensacola (P) a causeway (d) and a bridge (BR). Color tables for all the images are raw camera analog to digital units (ADUs). Red lines show 25 km scales for altitudes of 0, 15, and 87 km. (c) A plot of ADUs-3500 along the black line. This illustrates the relative change of airglow reflecting off the ground and water.

geolocation of the pixels, as well as illustrating the variety of features seen in the imagery. Figure 1c shows a plot along a vertical black line, shown in Figure 1b, of the intensity of the signal for these various features. Ocean water reflects the OH airglow poorly, low-altitude liquid water clouds reflect well, and ice clouds and airglow features appear at intermediate intensity. Features such as AGWs or KHIs are identified as originating from airglow emission altitudes using the NIRAC analysis technique (Hecht et al., 2023) from images 1 (Figure 1b) and 2. The lower left portion of Figure 1b, which shows Pensacola, illustrates PIANO's resolution as a highway bridge can be resolved. This image also shows high-altitude (above 80 km) KHI features present in the mostly clear skies well north of the hurricane Ian's eye-center.

2.2. PIANO Ian Imagery

Figure 2 shows a 4-image sequence, beginning at 040455.05 UT, with each separated by about 10 s and these capture the eyewall region. These panels have a number of color-coded arrows pointing at the features that are the main subject of this letter and are described in the caption. In particular, the yellow arrows show prominent eyewall features, which are also seen in GOES imagery presented below, and that are used to align the PIANO and

10.1029/2025GL116331

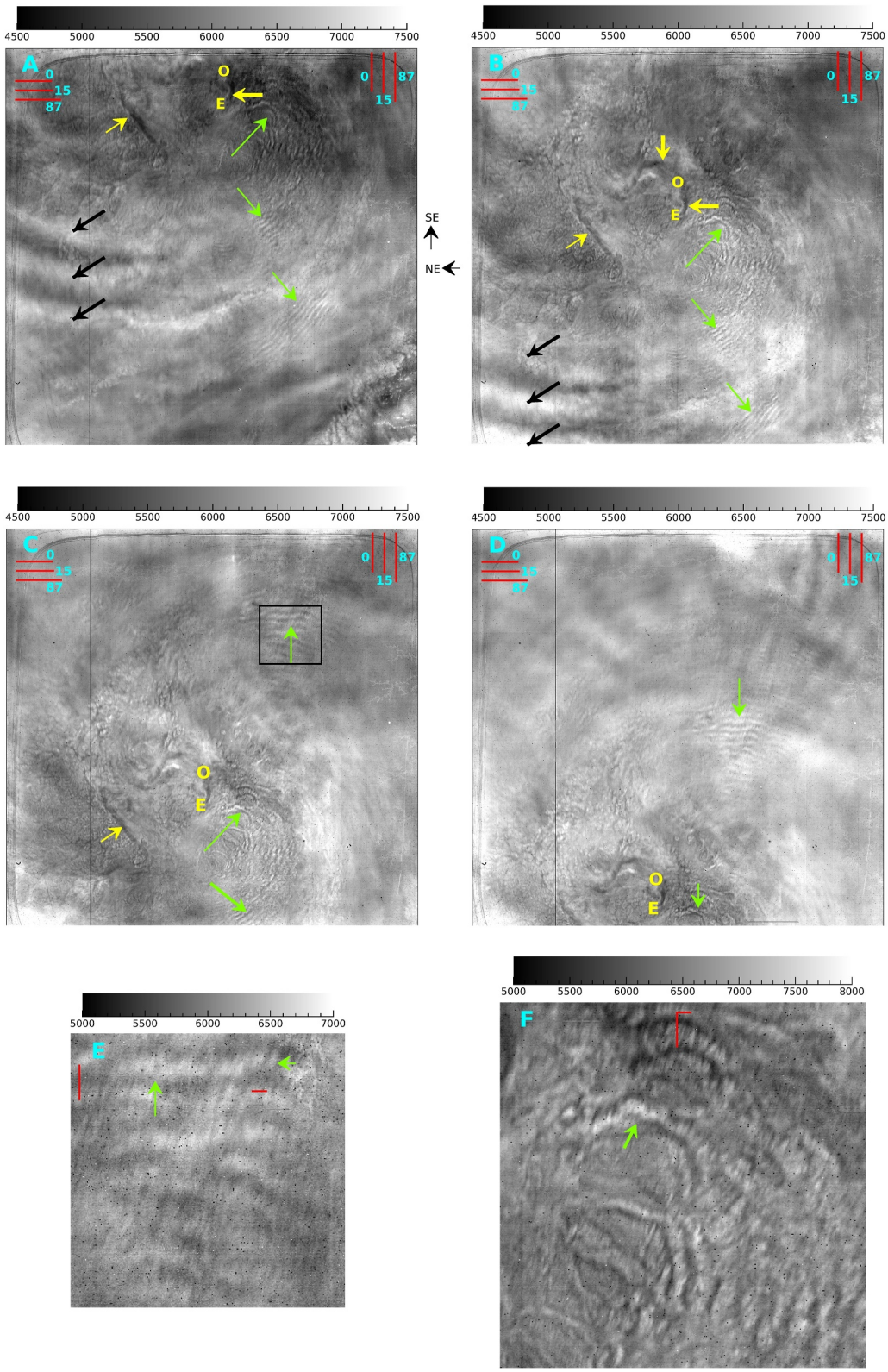

Figure 2. Panels (a–d) show images 8–11, respectively, and oriented with color tables and distance scales as in Figure 1b. Yellow arrows point to eyewall features. Yellow labels E and O l point to the end of one eyewall feature and the eye-center, respectively. Green and black arrows point to wave features at altitudes of ~15 km and ~87 km. A blue box and green arrow in panel (c) highlight NPWs that are expanded in panel (e). The other green arrows in panel (c) highlight horseshoe-shaped features (HSFs) expanded in panel (f). In panels (e, f) the redlines represent 5 and 2 km distances at a 15 km altitude.

GOES imagery. The green arrows highlight the Ian cloud wave features (NPWs) and horseshoe-shaped features (HSFs), while the black arrows point to high altitude AGW phase-fronts. As the ISS moves the features are displaced downwards in the images, but the AGWs are also displaced relative to the eyewall, consistent with being at a much higher altitude Figures 2e and 2f expand some of the wavelike features in the clouds to show structure perpendicular to their main phase-fronts.

To investigate this further and to confirm that the AGWs are occurring at high altitudes, well-separated from the hurricane cloud tops, Figure 3 is a multi-panel plot employing the NIRAC analysis technique. The top row shows two panels that show the same portion of the hurricane but from two different ISS locations (image 8 and 9) and hence from a different perspective. These portions of images 8 (Figure 2a) and 9 (Figure 2b) are selected to be aligned (in Figures 3a and 3b) to the edges of the yellow-highlighted eyewall features. Comparing Figures 3a and 3b the AGWs seem to be displaced with respect to eyewall, while the NPWs and horseshoe features appear to be more stationary. This is what would be expected if the AGWs are above 80 km, while the cloud features are below 20 km.

To confirm this, Figure 3c is the result of subtracting Figure 3b from Figure 3a and the AGW features become prominent because the cloud features are subtracted out. AGWs now are seen not only in the lower left corner but at other locations. Interestingly though, the upper set of the NPWs (labeled U in Figure 3a) disappears while the lower set (labeled L) still remains prominent.

Caution is needed when interpreting the subtracted images because of two issues. As discussed in Hecht et al. (2023) the NIRAC analysis technique will show apparent motion of features between the two images if they are at different heights, or if they move. For very short wavelength features even small phase front motion can result in noticeably incomplete subtraction between the two images. A complimentary and more robust analysis involves examining the distance and direction that the features moved. Thus, the features being discussed are affected by the analysis in somewhat different ways as discussed in a following section.

Finally Figure 1d is presented, analogous to Figure 1c, where now the selected portions of images 8 and 9 that show the same view are lined up at the AGW phase-fronts and then subtracted. The AGWs originating above 80 km almost completely disappear while the lower altitude cloud features are all prominent, reaffirming that these are not originating in the airglow layer.

2.3. PIANO and GOES-16 Imagery

Before discussing the characteristics of the NPW and AGW features a determination of their apparent heights is needed. To do this the PIANO data were plotted over the GOES height data as shown in Figure 4. The PIANO imagery (panel D) was rotated 47° to align with the Mercator geographic projection, and the center of the resultant image was set so that the prominent eyewall features of the PIANO image aligned with the GOES imagery. Additional interpolation was applied to the GOES imagery to produce the final figure.

1. The NPWs have λ_h of approximately 4 km. If one assumes the NPWs closest to the eyewall are at the same altitude as the rest of the Ian clouds then they are moving very slowly, at less than 10 ms^{-1}. The NPWs that are seen toward the bottom of the image of Figure 3a have phase-fronts that move about 3–4 pixels inward toward the eyewall. This amount of pixel displacement suggests a very fast motion, on the order of 100 ms^{-1} if they are at the same altitude as the cloud tops around the eyewall, or a slower motion if they are at a lower height. This is resolved using the cloud heights obtained from the GOES 16 analysis shown in Figure 4. The NPW features closest to and farthest from the eyewall, in Figures 3a and 4d, are at an altitude of 15.5 and 12.3 km, respectively. Thus, there is about a 3.2 km difference in altitude that accounts for about 2.5 pixels of the apparent motion. The residual motion is between 10 and 40 ms^{-1} toward the hurricane center. Both of these sets of NPWs appear to be located at the edge of a spiral arm where there is a change in altitude. The NPWs highlighted in Figure 2c (but not highlighted in Figure 4) are separated by about 6.8 km, but have prominent perpendicular structures that are separated by 2.2–2.8 km. Their altitudes are located around 16.3 km with velocities similar to the other NPWs.
2. The HSFs are separated by about 4 km, but they have fine-scale structure aligned perpendicular to the main phase. These structures have separations of between 0.5 and 2 km. These features appear to be moving about 50 ms^{-1} at ∼90° to the ISS direction of motion, so this apparent motion is not affected by cloud height.

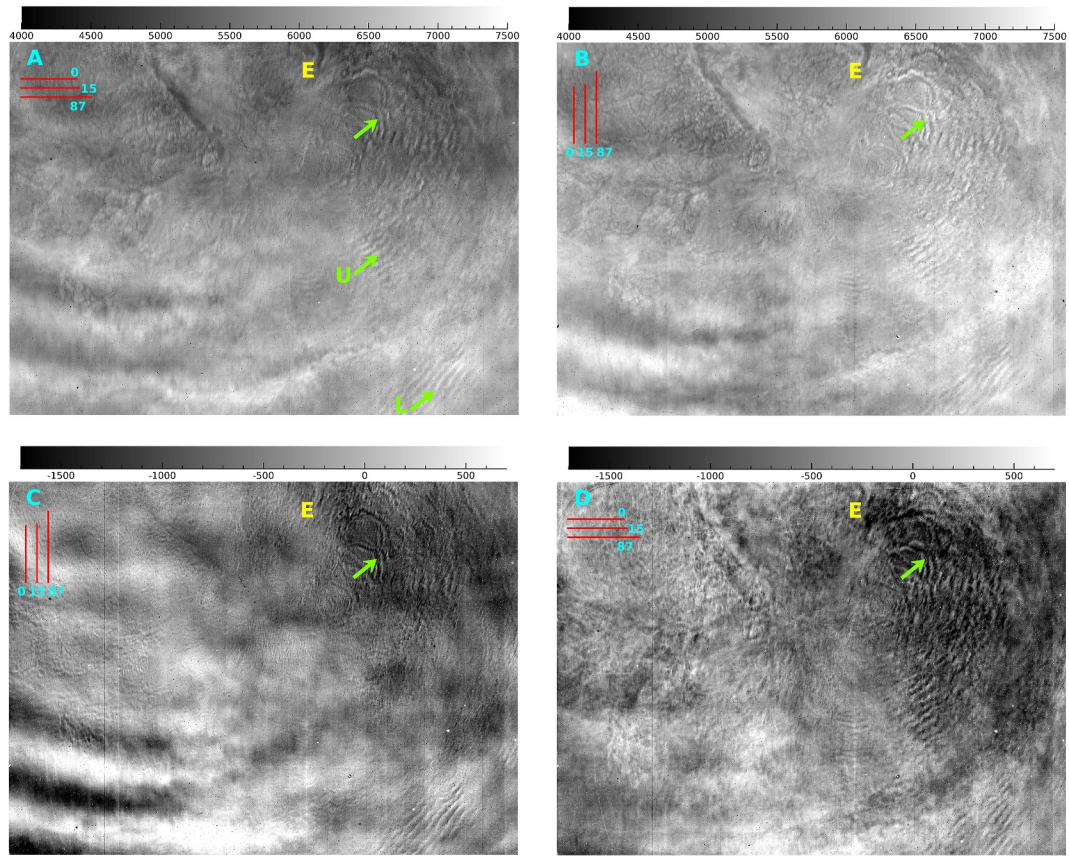

Figure 3. The orientation, distance, and color scales are as described in Figure 1b. See Hecht et al. (2023) for a complete explanation of the analysis shown here. (a) A portion of Figure 2a. The green arrow points to HSFs and NPWs that are labeled U and L, respectively. (b) A portion of Figure 2b, that is the same as in panel 2A but seen from a different ISS location. This is aligned so that the eyewall features highlighted by the yellow arrows of Figure 2b line up with those of panel (a). (c) Panel (a) minus panel (b). This mostly eliminates the cloud features and shows predominantly AGWs originating in the OH airglow layer (~87 km). (d) Similar to (c) but now two slightly different portions of Figures 2a and 2b, that are the same size as panels (a, b), but are chosen to align the AGW phase-fronts (black arrows in Figures 2a/2b), so this difference mostly eliminates the AGWs and shows features embedded in the hurricane clouds at altitudes from ~12–18 km.

3. The AGWs have λ_h of approximately 25 km. Using the cloud heights from the GOES image around the eyewall of ~17 km allows an estimate of how much a stationary AGW should be displaced if they are at the nominal 87 km altitude, typical for such features. Subtracting that number from the measured displacement allows the AGW velocity to be determined. However, because of the ISS pitch and the unknown exact altitude of the airglow layer these values fall between ~10 to 60 ms^{-1}. The direction is away from the eyewall.

3. Discussion

3.1. Hurricane Ian Cloud Features

3.1.1. NPWs

Features similar to the NPWs were first described in Black (1983) from analysis of photographs taken from Skylab in 1973. More recently, Nolan and Onderlinde (2022) noted similar features in numerical simulations, and were able to find a few supporting examples in visible satellite imagery. While additional examples have been found, they seem to be visible only in category 4 or 5 storms. In the simulations, the waves had very slow propagation speeds, generally less than 20 ms^{-1}, and horizontal wavelengths around 5 km. Nolan and Onderlinde (2022) suggest these are KHIs, and the PIANO observations presented here, which are the first to identify perpendicular structures, support this interpretation, at least from a morphological perspective. KHIs are known to sometimes develop secondary instability structures that are at right angles to the primary phase-fronts (Klaassen

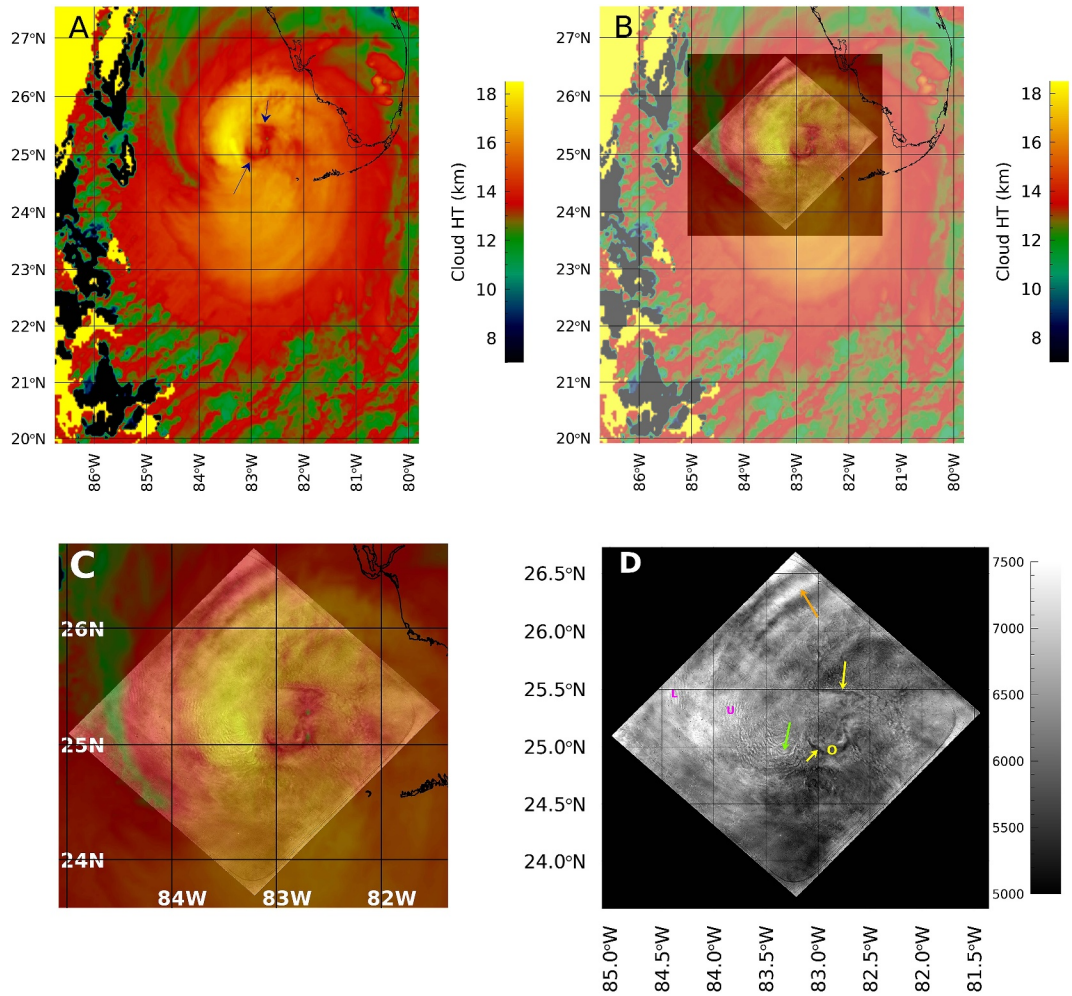

Figure 4. The GOES imagery for the Ian cloud heights at 0404 UT combined with PIANO image 9 with 260 m pixels. (a) GOES only at 0406 UT. The arrows (blue here instead of yellow for better visibility) point to features in the imagery that align with the same features seen in PIANO imagery (Figure 2b). The color-bar relates the colors to Ian cloud-top altitudes. (b) The GOES image is 40 percent transparent showing the PIANO image. The eyewall features in the PIANO image are lined up with the same features seen in the GOES image. The AGW features from PIANO seem to have a similar spiral nature as the Ian clouds. (c) An expanded view of panel (b). (d) PIANO image only but the same size as in panel (c). Yellow features and the green arrow are as described in Figure 2b. The NPW regions are the magenta U and L that are green in Figure 3a.

& Peltier, 1985, 1991), and such features are routinely seen in imaging of the MLT airglow. These secondary instabilities are often observed in the airglow to have wavelengths that are about one third to one fifth of the wavelength of the primary KHIs (Hecht et al., 2014, 2018), consistent with the NPWs and HSFs in this study. Variations in this ratio, or even the absence of secondaries have also been seen (Fritts, Baumgarten, et al., 2014; Hecht et al., 2014). Theoretically, the separation of the primaries is about 6–8 times that of the shear layer responsible for the KHI formation (Fritts, Wan, et al., 2014; Hecht et al., 2005) suggesting that the vertical extent of the shear layer producing the NPWs is about 0.5–1 km.

3.1.2. Horseshoe-Shaped Features (HSFs)

These features also show fine structures that appear perpendicular to the horseshoes. As the HSFs are moving at about 50 ms^{-1} around the top of the eyewall, we speculate that they are caused by convective updrafts advected by the very fast cyclonic flow in the lower eyewall which is then impinging on the stable tropopause leading to very strong vertical shear, KHI, and turbulence. The horseshoe shapes are the leading edges of the "upside down" gravity currents created by the rapidly moving convective outflows. Alternatively, the features could be

interpreted as "bow waves" generated by tall convective clouds pushing into the stratosphere. The features here are less well defined and suggest turbulent breakdown at the leading edge which is more similar to downbursts (e.g., Schumacher et al. (2023)).

3.2. AGWs in the Airglow Layer

To determine the origin of the AGWs we calculated the transit time for an AGW to travel from 20 to 80 km with no winds using simplified AGW ray tracing equations (Hecht et al., 2004) with a 40 ms^{-1} horizontal velocity wrt the ground, a value consistent with these and other observations (Hecht, 2004). We use model winds to calculate the intrinsic velocity. Available European Centre for Medium-Range Weather Forecasts (ECMWF) ERA5 reanalysis winds, in the direction of the AGW ($\sim 39°$ from north) are quite low, mostly below 5 ms^{-1} from 20 to 50 km. The AGW transit time is ~1 hr over an approximate horizontal distance of 150 km. The ECMWF wind uncertainties could increase the distance slightly, a few tens of kms, but larger AGW phase speeds would reduce the distance. Hence, as the distance of the two AGW phase-fronts from the center of the hurricane is between 130 and 190 km, and a few tens of kms further if generated 1–2 hr earlier, these results indicate that it is plausible that these AGWs did originate from close to the eyewall. While no visible time-lapse imagery was available during the period where the AGWs were being actively generated by the hurricane dynamics, it seems plausible that these features are segments of concentric or spiral waves generated by deep convection in the eyewall. These observed AGWs are morphologically similar to those previously observed from Hurricane Matthew in Miller et al. (2019), and from the NASA Atmospheric Infrared Sounder (AIRS) observations of stratospheric AGWs from tropical convection discussed in Tratt et al. (2018) and Yue et al. (2014).

4. Summary

Very-high spatial resolution nighttime imagery, with pixel footprints smaller than 100 m, was obtained by the PIANO OH airglow imager as the ISS orbital track passed over Hurricane Ian on 28 September 2022 during a period when the moon was down, and the storm was transitioning from category 4 to 5. The imagery revealed different fine-structured sets of wavelike features at the top of the hurricane clouds. One set included NPWs with horizontal wavelengths of about 4–7 km consistent with previous tropospheric modeling. Using GOES imagery it is shown that these features were not all at the same altitude, with some more than 3 km lower than the other two. Some NPWs had very fine perpendicular structure with a spacing close to one third of the primary phase-front spacing. A second set of features were horseshoe-shaped and like some of the NPWs they had very fine perpendicular structure separated by ~1 km. These fine-scale structures in the NPWs and horseshoe-shaped features are morphologically similar to secondary convective instabilities often seen in airglow imagery. This observed morphology strongly suggests that the NPWs, and possibly the HSFs, are plausibly KHIs that sometimes develop secondary convective instabilities. This supports the suggestion by Nolan and Onderlinde (2022) from their modeling of the NPWs that the short-horizontal wavelength features are KHIs. Finally, some larger scale AGWs with horizontal wavelengths of about 25 km are seen in the PIANO imagery and these are present in the OH emission layer located above 80 km altitude. Using available wind data these waves were plausibly generated by the hurricane, 1–2 hr earlier, close to the eyewall. Thus, it is likely that dynamic processes at the eyewall were responsible for the AGWs seen above 80 km.

Data Availability Statement

All the PIANO data and the GOES data that are used to produce the overlays and the IDL code are available at zenodo.org (Hecht & Gelinas, 2025). For these plots we used Interactive Data Language (IDL) plotting routines and warped both GOES (500 × 500 pixel) and PIANO imagery to a Mercator projection (Hecht & Gelinas, 2025). The latitude and longitude for each GOES channel-16 2-km pixel were obtained from the University of Wisconsin archives. The cloud top heights for each pixel were obtained from the Amazon archive image with 250 × 250 4-km pixels. The height images were interpolated to a 500 × 500 array, and the corresponding pixel latitude and longitudes were then obtained from the Wisconsin files. The prominent eyewall features in both GOES arrays verified that this method was valid. Specifically, NOAA Geostationary Operational Environmental Satellites (GOES) 16 data were accessed from registry.opendata.aws/noaa-goes and from inventory.ssec.wisc.edu. The ECMWF data (Hersbach et al., 2023) were obtained from the Copernicus Climate Store cds.climate.copernicus.eu.

Acknowledgments
JHH and LJG were supported by The Aerospace Corporation's SERPA program and by NSF through Grant AGS-1911952. DSN was supported by the NSF through Grant AGS-2334173.

References

Black, P. (1983). Tropical storm structure revealed by stereoscopic photographs from skylab. *Advances in Space Research*, *2*(6), 115–124. https://doi.org/10.1016/0273-1177(82)90131-4306

Bucci, L., Alaka, L., Hagen, A., Delgado, S., & Beven, J. (2023). *Hurricane Ian (Al092022) 23-3-September 2022, national hurricane center tropical cyclone report*. NHC Tech. Rep. (Vol. 72). Retrieved from https://www.nhc.noaa.gov/data/tcr/AL092022_Ian.pdf

Fritts, D. C., Baumgarten, G., Wan, K., Werne, J., & Lund, T. (2014). Quantifying Kelvin-Helmholtz instability dynamics observed in noctilucent clouds: 2. Modeling and interpretation of observations. *Journal of Geophysical Research: Atmospheres*, *119*(15), 9359–9375. https://doi.org/10.1002/2014JD021833

Fritts, D. C., Wan, K., Werne, J., Lund, T., & Hecht, J. H. (2014). Modeling the implications of Kelvin-Helmholtz instability dynamics for airglow observations. *Journal of Geophysical Research: Atmospheres*, *119*(14), 8858–8871. https://doi.org/10.1002/2014JD021737

Gelinas, L. J., Hecht, J. H., & Rudy, R. J. (2024). The near-infrared airglow camera on the international space station. *Journal of Atmospheric and Oceanic Technology*, *41*(2), 147–160. https://doi.org/10.1175/JTECH-D-23-0069.1

Hecht, J. H. (2004). Instability layers and airglow imaging. *Reviews of Geophysics*, *42*(1), RG1001. https://doi.org/10.1029/2003RG000131

Hecht, J. H., Fritts, D. C., Wang, L., Gelinas, L. J., Rudy, R. J., Walterscheid, R. L., et al. (2018). Observations of the breakdown of mountain waves over the Andes lidar observatory at Cerro Pachon on 8/9 July 2012. *Journal of Geophysical Research: Atmospheres*, *123*(1), 276–299. https://doi.org/10.1002/2017JD027303

Hecht, J. H., & Gelinas, L. J. (2025). High-spatial resolution space-based observations in the upper troposphere and upper mesosphere of wavelike features produced by Hurricane Ian [Dataset]. *Zenodo*. https://doi.org/10.5281/zenodo.16749084

Hecht, J. H., Gelinas, L. J., Rudy, R. J., & Walterscheid, R. L. (2023). Atmospheric gravity wave and instability observations from the International Space Station using the Near InfraRed Airglow Camera (NIRAC). *Journal of Geophysical Research: Atmospheres*, *128*(19), e2023JD039070. https://doi.org/10.1029/2023JD039070

Hecht, J. H., Kovalam, S., May, P. T., Mills, G., Vincent, R. A., Walterscheid, R. L., & Woithe, J. (2004). Airglow imager observations of atmospheric gravity waves at Alice Springs and Adelaide, Australia during the Darwin Area Wave Experiment (DAWEX). *Journal of Geophysical Research*, *109*(D20), D20S05. https://doi.org/10.1029/2004JD004697

Hecht, J. H., Liu, A. Z., Walterscheid, R. L., & Rudy, R. J. (2005). Maui mesosphere and lower thermosphere (Maui malt) observations of the evolution of Kelvin-Helmholtz billows formed near 86 km altitude. *Journal of Geophysical Research*, *110*(D9), D09S10. https://doi.org/10.1029/2003JD003908

Hecht, J. H., Wan, K., Gelinas, L. J., Fritts, D. C., Walterscheid, R. L., Rudy, R. J., et al. (2014). The life cycle of instability features measured from the Andes Lidar Observatory over Cerro Pachon on 24 March 2012. *Journal of Geophysical Research: Atmospheres*, *119*(14), 8872–8898. https://doi.org/10.1002/2014JD021726

Hersbach, H., Bell, B., Berrisford, P., Biavati, G., Horányi, A., Muñoz Sabater, J., et al. (2023). ERA5 hourly data on pressure levels from 1940 to present. *Copernicus Climate Change Service (C3S) Climate Data Store (CDS)*. https://doi.org/10.24381/cds.bd0915c6

Hoffmann, L., Wu, X., & Alexander, M. J. (2018). Satellite observations of stratospheric gravity waves associated with the intensification of tropical cyclones. *Geophysical Research Letters*, *45*(3), 1692–1700. https://doi.org/10.1002/2017GL076123

Klaassen, G. P., & Peltier, W. R. (1985). The onset of turbulence in finite-amplitude Kelvin–Helmholtz billows. *Journal of Fluid Mechanics*, *155*, 1–35. https://doi.org/10.1017/S0022112085001690

Klaassen, G. P., & Peltier, W. R. (1991). The influence of stratification on secondary instability in free shear layers. *Journal of Fluid Mechanics*, *227*, 71–106. https://doi.org/10.1017/S0022112091000046

Miller, S. D., Straka, I., William, C., Yue, J., Seaman, C. J., Xu, S., et al. (2019). The dark side of Hurricane Matthew: Unique perspectives from the VIIRS day/night band. *Bulletin of the American Meteorological Society*, *99*(12), 2561–2574. https://doi.org/10.1175/BAMS-D-17-0097.1

Nolan, D. S., & Onderlinde, M. J. (2022). The representation of spiral gravity waves in a mesoscale model with increasing horizontal and vertical resolution. *Journal of Advances in Modeling Earth Systems*, *14*(8), e2022MS002989. https://doi.org/10.1029/2022MS002989

Nolan, D. S., & Zhang, J. A. (2017). Spiral gravity waves radiating from tropical cyclones. *Geophysical Research Letters*, *44*(8), 3924–3931. https://doi.org/10.1002/2017GL073572

Schumacher, R. S., Childs, S. J., & Adams-Selin, R. D. (2023). Intense surface winds from gravity wave breaking in simulations of a destructive macroburst. *Monthly Weather Review*, *151*(3), 775–793. https://doi.org/10.1175/MWR-D-22-0103.1

Tratt, M., David, Hackwell, J. A., Valant-Spaight, B. L., Walterscheid, R. L., Gelinas, L. J., et al. (2018). Ghost: A satellite mission concept for persistent monitoring of stratospheric gravity waves induced by severe storms. *Bulletin America Meteorology Social*, *99*(9), 1813–1828. https://doi.org/10.1175/BAMS-D-17-0064.1

Wright, C. J. (2019). Quantifying the global impact of tropical cyclone-associated gravity waves using HIRDLS, MLS, SABER and IBTrACS data. *Quarterly Journal of the Royal Meteorological Society*, *145*(724), 3023–3039. https://doi.org/10.1002/qj.3602

Xu, S., Yue, J., Xue, X., Vadas, S. L., Miller, S. D., Azeem, I., et al. (2019). Dynamical coupling between Hurricane Matthew and the middle to upper atmosphere via gravity waves. *Journal of Geophysical Research: Space Physics*, *124*(5), 3589–3608. https://doi.org/10.1029/2018JA026453

Yue, J., Miller, S. D., Hoffmann, L., & Straka, W. C. (2014). Stratospheric and mesospheric concentric gravity waves over Tropical Cyclone Mahasen: Joint AIRS and VIIRS satellite observations. *Journal of Atmospheric and Solar-Terrestrial Physics*, *119*, 83–90. https://doi.org/10.1016/j.jastp.2014.07.003